Local Data Assimilation in Specification of Open Boundary Conditions

I. SHULMAN

Center for Marine Sciences, University of Southern Mississippi, Stennis Space Center, Mississippi

(Manuscript received 2 March 1995, in final form 26 December 1995)

ABSTRACT

A data assimilation approach to specify open boundary conditions is proposed. The boundary values are determined from the solution of the special optimization problem: minimization of the difference between the model and reference boundary values under the integral constraints on the open boundary. These constraints represent the energy, momentum, and mass fluxes through the open boundary. Reference values represent the a priori knowledge about the boundary values. They might be derived from observations, results of another model run, or from another approach to the specification of open boundary conditions. Optimized open boundary conditions are presented in detail for the barotropic case and when only one integral constraint is considered: energy flux through the open boundary. It is shown that well-known radiation-type boundary conditions introduced by Reid and Bodine, and Flather, are special cases of the derived optimized conditions. The results of application of the proposed boundary conditions are demonstrated in the modeling of tidal and wind-driven circulation for a channel and for the northern part of the Adriatic Sea. The results of studies of the model predictions' sensitivity to errors in the reference values used in the boundary conditions are presented. The applications of optimized open boundary conditions show a significant reduction in errors when compared to the commonly used, nonoptimized schemes.

1. Introduction

With the rapidly increasing amount of available observations, results of model simulations, and newly gained knowledge of physical processes, the development of data assimilation methods is in great demand. One of the areas of application of data assimilation methods is the specification of open boundary conditions (OBCs) for limited-area models. The use of data assimilation techniques improves the model predictions and avoids the ill-posed, point-wise treatment of OBCs (Bennett 1992, 1994; Oliger and Sundstrom 1978). In many data assimilation techniques of specifying OBCs, the latter are considered as control parameters. In this case, OBCs are chosen in such a way as to simultaneously provide the best fit to the governing equations and to the observations (e.g., Bennett 1992, 1994; Zou et al. 1993; Seiler 1993, etc.). The best fit means the minimization of the norm of the deviation between model results and observations. Thus, the interior solution and the available observations are used to calculate the variables on the open boundary. The main restriction of this approach is the need for significant amounts of computer time and memory.

In Shulman and Lewis (1994, 1995), OBCs are chosen by combining the model dynamics with the data assimilation only on the open boundary and its vicinity. It was shown that many well-known, radiation-type OBCs are special cases of the optimized OBCs obtained. The solution of this local data assimilation scheme was easily derived. Therefore, this approach does not significantly impact the computational time and the required memory. At the same time, the comparison between the Reid and Bodine formulation and the optimized version of this condition showed that optimization provides much better results in modeling tidal constituents.

In section 2, we describe the general formulation of the local data assimilation approach to specification of OBCs and provide the detailed description of the barotropic case. The applications of optimized OBCs are demonstrated for the cases of the idealized channel and the Adriatic Sea. The results of tidal and wind-driven simulations as well as sensitivity studies are presented and discussed in sections 3 and 4.

2. Derivation of the optimized open boundary conditions

Let vector $\mathbf{X}$ be the variables that we are to specify on the open boundary (sea surface height, velocity, temperature, salinity, etc.). Suppose we know some reference value of vector $\mathbf{X}$, which we denote as vector $\mathbf{X}^o$. The reference values of boundary variables in $\mathbf{X}^o$ can be estimated from available observations, another nu-

Corresponding author address: Dr. Igor Shulman, Center for Ocean and Atmospheric Modeling, University of Southern Mississippi, Building 1103, Rm. 249, Stennis Space Center, MS 39529.

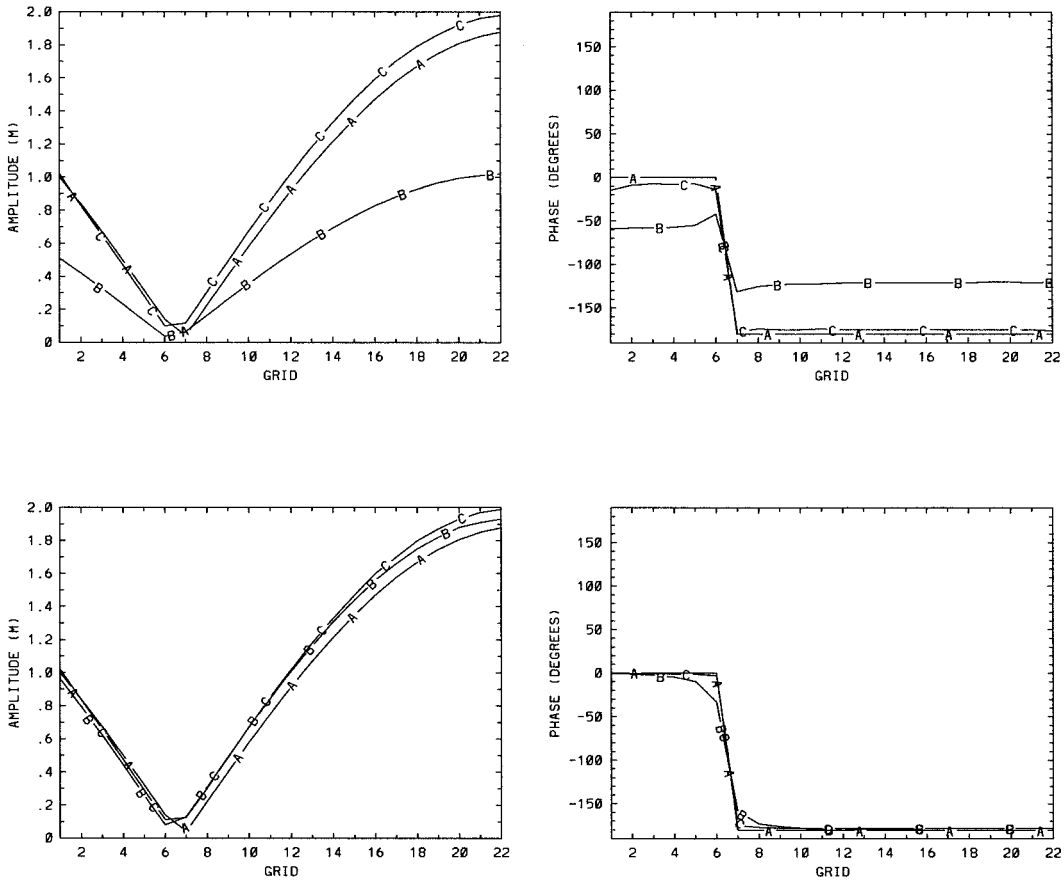

FIG. 1. Analytical solution and results of channel simulations with RB and ORB conditions (top) and FL and OFL conditions (bottom). Curve A is the analytical solution, curve B is the result of application of the RB (top) and the FL (bottom) conditions, and curve C is the result of application of the ORB (top) and the OFL (bottom) conditions.

merical simulation, and approximations based on the governing physics. We introduce the function $J(\mathbf{X}, \mathbf{X}^o) \geq 0$, which represents the difference between model and reference values of variables on the open boundary. Let P_t be the energy flux through an open boundary, which results from the difference in values of vectors $\mathbf{X}$ and $\mathbf{X}^o$. Accordingly, let M_t be the mass flux and F_t be the momentum flux through the open boundary, which results from the difference in values of vectors $\mathbf{X}$ and $\mathbf{X}^o$. If we suppose that we know some estimates of P_t, M_t, and F_t, we might choose the boundary values (vector $\mathbf{X}$) from the following optimization problem:

$$\min_{\mathbf{X}} J(\mathbf{X}, \mathbf{X}^o), \tag{1}$$

$$A(\mathbf{X}, \mathbf{X}^o) = P_t, \tag{2}$$

$$B(\mathbf{X}, \mathbf{X}^o) = M_t, \tag{3}$$

$$C(\mathbf{X}, \mathbf{X}^o) = F_t, \tag{4}$$

where A, B, and C are operators for calculating energy, mass, and momentum fluxes. Thus, we choose open boundary values by minimizing the deviation between the reference and model boundary values under the integral constraints representing the energy, mass, and momentum fluxes. Solving (1)–(4) is a very complicated problem, and different approaches can be used. Each of these approaches has to take into account that the estimated P_t, M_t, F_t, and reference values may contain errors.

In this paper, we consider the minimization of (1) under only constraint (2) for vertically averaged, hydrostatic equations. Let S is the open boundary of the model domain D, u_n and η are the vertically averaged outward normal velocity and the sea surface elevation on the open boundary, H is the depth, and g is the gravitational constant. Suppose that we have some reference values of sea surface elevation on the open boundary in the form of η^o and some reference values of the outward normal velocity in the form of u_n^o. For the vertically averaged, hydrostatic problem, the minimization of (1) under constraint (2) can be written in the following form:

$$\min_{\eta}\left[J = \frac{g}{2}\int_S (gH)^{1/2}(\eta - \eta^o)^2\, ds\right], \tag{5}$$

$$-g\int_S H(\eta - \eta^o)(u_n - u_n^o)\, ds = P_t, \tag{6}$$

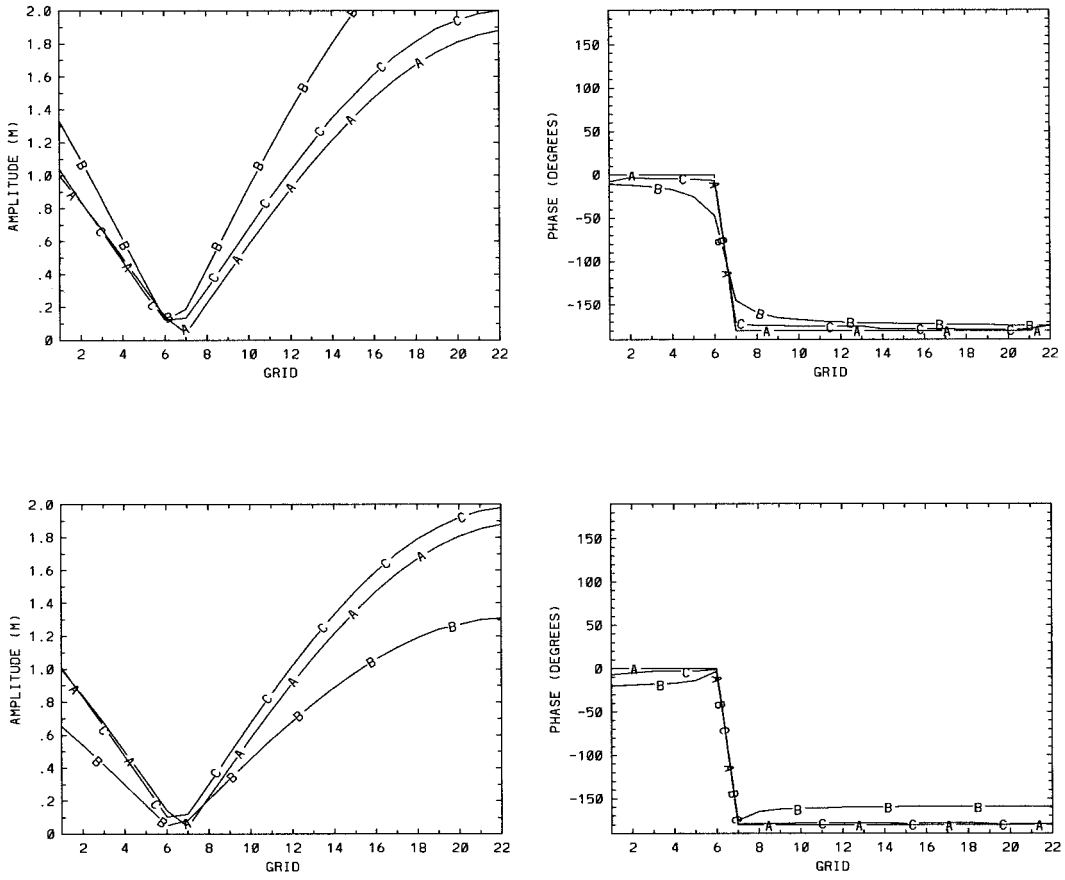

FIG. 2. Analytical solution and results of channel simulations with FL and OFL conditions. The amplitude of the reference velocity u_n^o is increased by 50% (top) and reduced by 50% (bottom). Curve A is the analytical solution, B is the result of application of the FL condition, and C is the result of application of the OFL condition.

where P_t is as previously defined and (6) is the energy flux resulting from the differences in model and reference values of sea surface elevation and velocity. In a real-world situation, P_t, η^o, and u_n^o contain some errors. For this reason, to solve problems (5) and (6), we employ the regularization method (Sabatier 1987; Parker 1994). This approach provides the determination of the solutions of (5) and (6) that will be stable with respect to the above-mentioned errors. In this case, problems (5) and (6) are reduced to the following minimization problem:

$$\min_{\eta}\left\{\frac{1}{2}\left[P_t + g\int_S H(\eta - \eta^o)(u_n - u_n^o)\,ds\right]^2 + \gamma\frac{g}{2}\int_S (gH)^{1/2}(\eta - \eta^o)^2\,ds\right\}, \tag{7}$$

where γ is a parameter of regularization. The solution of (7) has the following form:

$$u_n - u_n^o = \left(\frac{g}{H}\right)^{1/2}\frac{(\eta - \eta^o)}{\lambda_t}, \tag{8}$$

where

$$\lambda_t = -\frac{P_t}{g^{1/2}\displaystyle\int_S H^{3/2}(u_n - u_n^o)^2\,ds + \gamma}. \tag{9}$$

To determine boundary conditions from (8) and (9), we have to choose a value for the parameter γ. There are many different approaches to choosing γ. Most of them rely on the estimate of the error in the input data. In most cases, we do not know the norms of the errors in the estimates of P_t and the reference values. Moreover, these norms will change from time to time. Therefore, the attractive approaches are the ones that do not require the a priori knowledge of the error norms. In the appendix, we briefly describe an approach of choosing the value of γ that provides the maximum of the entropy integral. This approach was used in this study.

Condition (8) can be considered as a method of boundary value relaxation toward the reference values. The condition has a coefficient of relaxation λ_t that changes over time and provides the adaptation of the boundary values to the change in the energy flux through the open boundary. Condition (8) is a modification of the boundary condition introduced in Flather (1976),

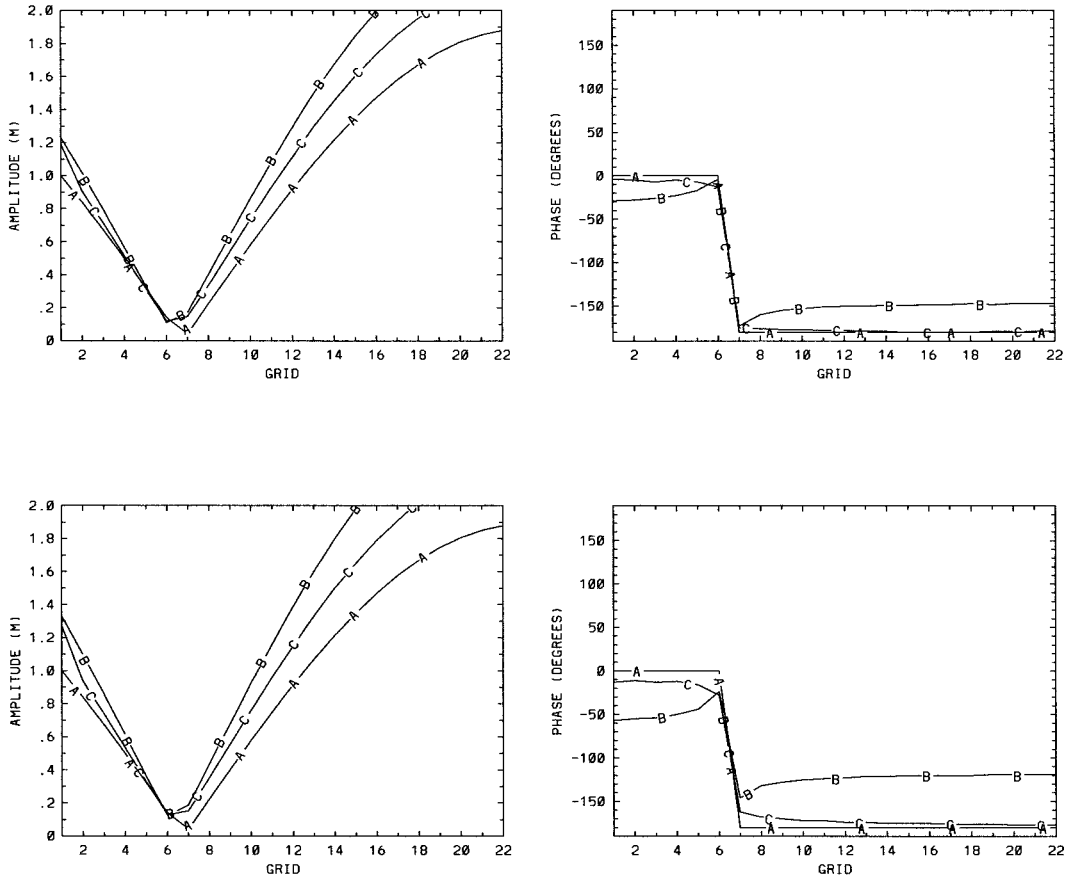

FIG. 3. Analytical solution and results of channel simulations with FL and OFL conditions. The phase shift of the reference velocity u_n^o with respect to the reference sea surface height η^o is equal to 45° (top) and 0° (bottom). Curve A is the analytical solution, B is the result of application of the FL condition, and C is the result of application of the OFL condition.

when $\lambda_t = 1$. This condition has been employed by many researchers (e.g., Oey and Chen 1992; Davies and Lawrence 1994; etc.).

When $u_n^o = 0$, condition (8) becomes

$$u_n = \left(\frac{g}{H}\right)^{1/2} \frac{(\eta - \eta^o)}{\lambda_t}. \tag{10}$$

Note that condition (10), when $\lambda_t = 1$, is a modification of the boundary condition introduced by Reid and Bodine (1968). Below, the conditions (8) and (10), when λ_t is calculated from (9), are called optimized versions of the Flather and the Reid and Bodine boundary conditions and denoted correspondingly as OFL and ORB. The standard versions of the Flather and Reid and Bodine conditions are denoted as FL and RB.

3. Channel simulations with optimized OBCs

Consider a flat-bottom, frictionless, channel closed at one end (Shulman and Lewis 1994, 1995). The channel is forced at the other end by surface height oscillations at the M_2 tidal frequency with the amplitude of 1 m [function η^o in (8) and (10)]. The length of the channel is 335 km and the depth is 50 m. There are 23 grid points along the channel (23rd is a wall). In Fig. 1 (top) we reproduced the analytical solution plus the results of the simulations for RB and ORB presented in Shulman and Lewis (1995). One can see that the error in predicting the amplitude is around 60% and the phase offset is around 60° for the RB condition. At the same time, the ORB condition almost entirely eliminated errors in predicted amplitudes while more than halving the errors in predicted phases. We conducted the same experiments with the FL and OFL conditions. The function u_n^o was calculated from the analytical solution for this problem (Officer 1976). The results of the simulations are shown in Fig. 1 (bottom), and they are very close for both FL and OFL conditions.

The results of the simulations with the RB condition can be interpreted as the results of an application of the FL condition with the estimate of the u_n^o being equal to zero [see (8) and (10), when $\lambda_t = 1$]. This suggests that the FL condition may be sensitive to errors in data used to construct the reference values of the sea surface el-

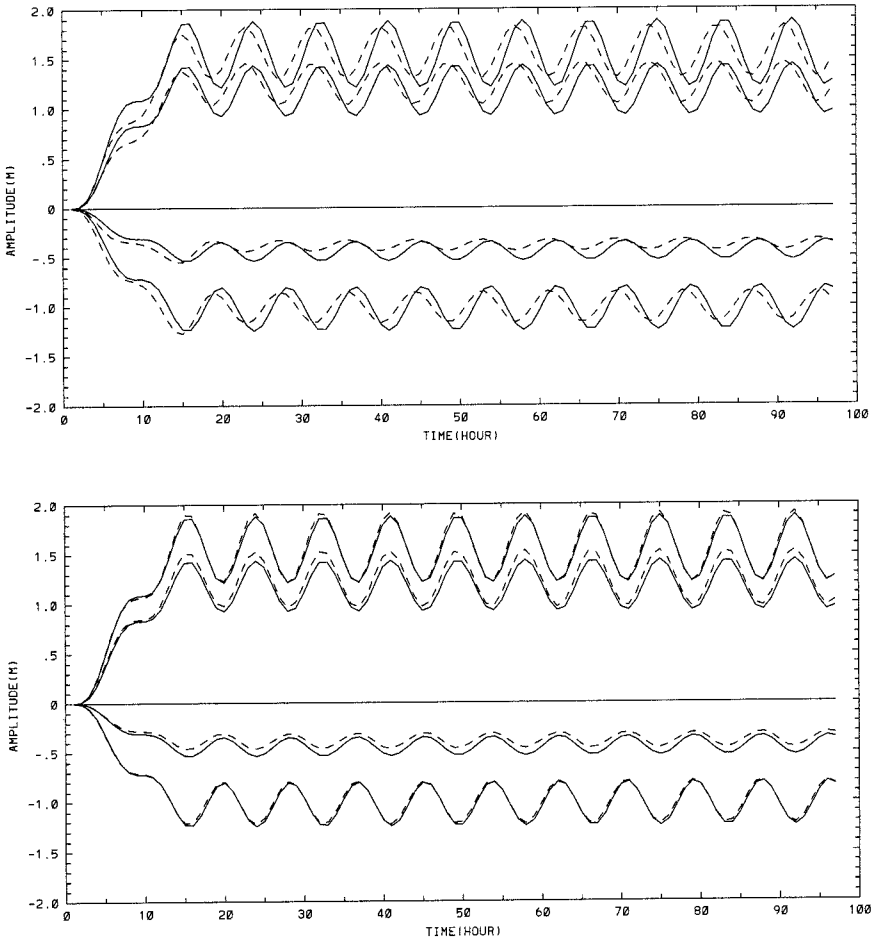

FIG. 4. Time series of sea surface elevation at four locations in the channel. The solid line is the analytical solution, and the dashed line is the model result with the application of the RB condition (top) and the ORB (bottom).

evation and velocity (functions η^o and u_n^o). To test this we conducted four experiments. In the first experiment, the amplitude of the reference velocity u_n^o is increased by 50%. The results of simulations with FL and OFL conditions are shown in Fig. 2 (top). The maximum error in predicting the amplitudes reaches 41.5% for FL. At the same time, the optimized version of the Flather condition has a maximum error of only 6.4%. In the second experiment, the amplitude of u_n^o is reduced by 50%. The results of simulations are shown in Fig. 2 (bottom), and the maximum error of predicted amplitudes is 30.3% for FL but only 5.3% for OFL.

From the analytical solution (Officer 1976), the correct phase shift for u_n^o with respect to η^o is 90°. In the third and fourth experiments, we introduced errors in the phase of u_n^o. The results of simulations with FL and OFL conditions when the phase shift of u_n^o with respect to η^o equals 0° and 45° are shown in Fig. 3. The use of the FL condition produces the maximum phase offset from the analytical solution equaling 60°. However, the maximum phase offset is only 12° when we use the OFL condition. The results of the numerical simulations clearly show that predictions using the FL condition are very sensitive to the errors in reference values of the sea surface elevation and velocity. But, the application of the optimized Flather condition results in much smaller errors.

To test the optimized OBCs for reproducing wind-driven circulation, we conducted a simulation for the channel with some simple wind forcing. Let us consider the following simple analytical problem to get an idea about the results expected. Suppose we have the same channel as before, but closed at both sides. Neglecting the nonlinear terms and bottom friction, the flow can be described by the following system of equations:

$$\frac{\partial u}{\partial t} = -g\frac{\partial \eta}{\partial x} + \frac{W}{H\rho}, \tag{11}$$

$$\frac{\partial \eta}{\partial t} = -H\frac{\partial u}{\partial x}, \tag{12}$$

where W is the wind stress. We have the following initial and boundary conditions:

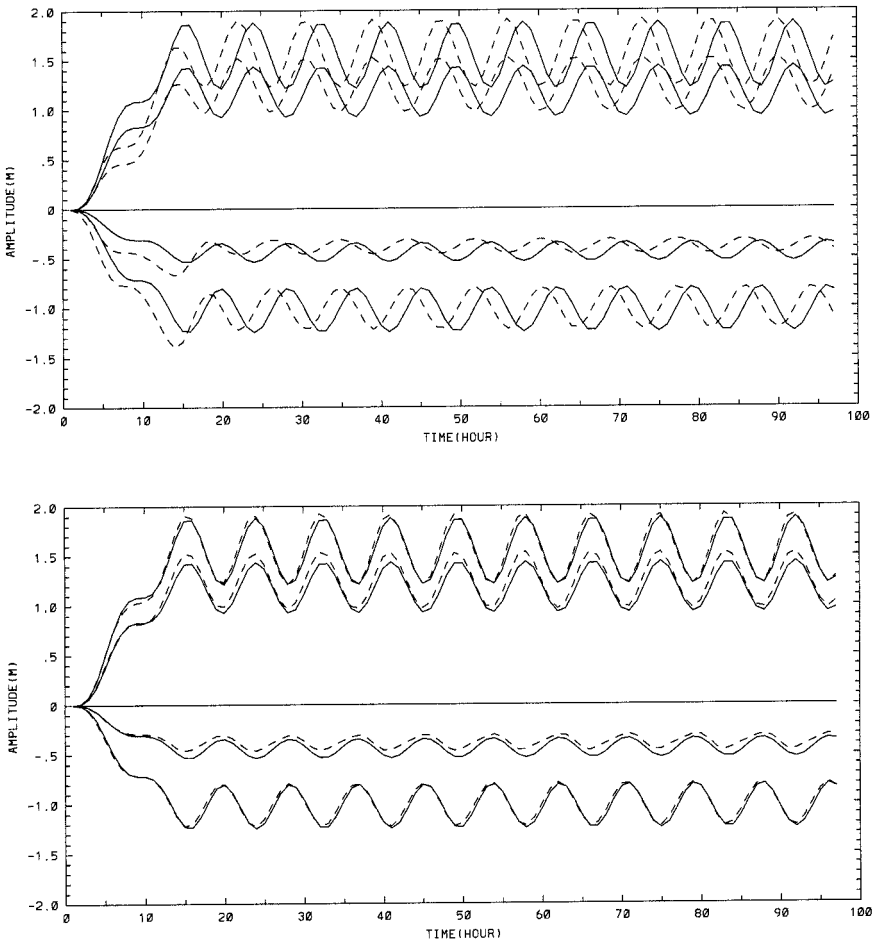

FIG. 5. Same as Fig. 4 but the dashed line is the model result with the application of the FL condition (top) and the OFL (bottom).

TABLE 1. Observed and model-predicted amplitudes (cm) and phases (degrees, relative to UTC) for the M_2 tide in the northern Adriatic Sea based on a simulation using the finer grid model of the Mediterranean Sea.

	Model		Observed		Difference (%)	
Station	Amplitude	Phase	Amplitude	Phase	Amplitude	Phase
P. P. Vecchia	19.7	260.9	22.3	257.0	−12.1	1.5
Rovinj	15.2	241.4	19.3	242.5	−21.2	−0.5
P. Corsini	13.8	270.6	15.5	274.0	−10.9	−1.2
Pesaro	9.4	285.1	12.8	288.0	−26.6	−1.0
Ancona	5.2	304.4	6.0	316.0	−13.3	11.6
Pula	10.9	231.7	15.1	236.3	−27.8	−2.0

TABLE 2. Observed and model-predicted amplitudes (cm) and phases (degrees, relative to UTC) for the M_2 tide in the northern Adriatic Sea based on a simulation using the coarser grid model of the Mediterranean Sea.

	Model		Observed		Difference (%)	
Station	Amplitude	Phase	Amplitude	Phase	Amplitude	Phase
P. P. Vecchia	53.5	275.2	22.3	257.0	140.0	7.1
Rovinj	51.3	265.5	19.3	242.5	166.0	9.5
P. Corsini	27.4	289.7	15.5	274.0	76.7	5.7
Pesaro	17.3	304.1	12.8	288.0	35.1	5.6
Ancona	6.3	33.6	6.0	316.0	5.0	24.6
Pula	25.5	246.2	15.1	236.3	68.8	4.1

$$u|_{x=0} = 0, \qquad u|_{x=L} = 0, \tag{13}$$

$$u(x, 0) = \eta(x, 0) = 0, \tag{14}$$

where L is the length of the channel and ρ is the water density. Suppose that W has the following form:

$$W(x, t) = \phi(t) \sin\frac{\pi x}{L}, \tag{15}$$

where

$$\phi(t) = \begin{cases} at, & t \le \epsilon \\ a\epsilon, & \epsilon \le t \le T. \end{cases}$$

Therefore, we have the wind linearly increasing with time and then constant after time ϵ. The analytical solution of problem (11)–(15) has the following form:

$$u(x, t) = \theta(t) \sin\frac{\pi x}{L}, \tag{16}$$

$$\theta(t) = \begin{cases} \dfrac{a(1 - \cos\beta t)}{(H\rho\beta^2)}, & t \le \epsilon \\ \dfrac{2a \sin(\beta\epsilon/2) \sin\beta(t - \epsilon/2)}{(H\rho\beta^2)}, & \epsilon \le t \le T \end{cases}$$

$$\eta(x, t) = \psi(t) \cos\frac{\pi x}{L}, \tag{17}$$

$$\psi(t) = \begin{cases} (-\pi a t/L\rho\beta^2) + (a\pi/L\rho\beta^3) \sin\beta t, & t \le \epsilon \\ (-\pi a\epsilon)/(L\rho\beta^2) + 2a\pi \sin(\beta\epsilon/2) \cos\beta(t - \epsilon/2)/(L\rho\beta^3), & \epsilon \le t \le T, \end{cases}$$

where

$$\beta = \frac{\pi}{L}(gH)^{1/2}.$$

We choose the following values for the unknown parameters: $L = 335\,000$ m, $\rho = 1025$ kg m^{-3}, $H = 50$ m, $\epsilon = \frac{1}{2}$ day $= 43\,200$ s, $T = 4$ days, $a = 1.7 \times 10^{-4}$. The value of a corresponds to wind stress linearly increasing from zero to 7.35 N m^{-2} during a half day [if we suppose the drag coefficient is 2.6×10^{-3} (Hellerman and Rosenstein 1983), the maximum wind speed is around 48 m s^{-1}].

The model run reproduced reasonably well the analytical solution for the closed channel. To test the optimized OBCs, we cut our computational domain on one side, removed five grid cells, and considered a sixth point as the open boundary. On the open boundary, the reference values of the sea surface elevation η^o and velocity u_n^o were taken from the analytical solutions in (16) and (17). The analytical solution at four grid points along the channel and the results of the simulations with the RB, ORB, FL, and OFL conditions are shown in Figs. 4 and 5. The optimized versions of boundary conditions reproduced the analytical solution very well, and the results are very close for both optimized conditions. At the same time, the usual versions of the Reid and Bodine and Flather conditions produced significant deviations from the analytical solution.

4. Modeling tidal and wind-driven circulation in the northern part of the Adriatic Sea

The model used in this study is the σ-coordinate, explicit version of the Princeton ocean model (Blumberg and Mellor 1987). This model is a three-dimensional, free-surface, primitive equations model. It includes the Mellor–Yamada turbulence closure submodel, and Smagorinsky diffusivity scheme for horizontal diffusion. The model uses a mode-splitting technique: the separation of vertically integrated equations (external, barotropic mode) from the vertical structure equations (internal, baroclinic mode). In this study, the simulations were conducted using only the barotropic mode of the model. For additional information on the model, the reader is referred to Blumberg and Mellor (1987).

Two orthogonal curvilinear grids were used that cover the entire Mediterranean Sea. The first grid had a relatively fine mesh with 441×141 grid points in the horizontal and a grid size ranging from 8 to 12 km in the Adriatic Sea. The second grid had a relatively coarse mesh (221×71 grid points) with a grid size ranging from 32 to 61 km in the Adriatic Sea area. The comparison of tidal observations in the region of the northern Adriatic Sea with the results of the simulation using the fine grid model are shown in Table 1. These results provide a good approximation of the observations at six tidal stations: Porto Piave Vecchia, 45.29°N, 12.34°E; Rovinj, 45.05°N, 13.38°E; Porto Corsini, 44.30°N,

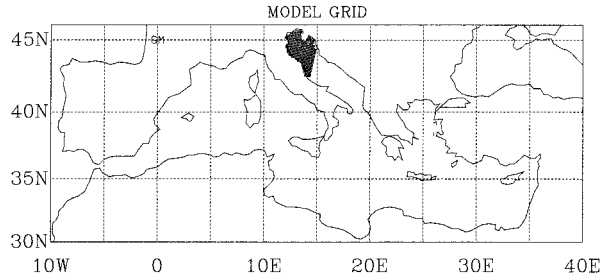

FIG. 6. Limited-area model of the northern part of the Adriatic Sea.

12.17°E; Pesaro, 43.55°N, 12.55°E; Ancona, 43.37°N, 13.30°E; and Pula, 44.52°N, 13.50°E. To quantify the errors, we use a weighted average percent error for these six northern Adriatic Sea stations. The average error is 18.6% for amplitudes and 1.7% for phase. The predictions of M_2 tides in the northern Adriatic using the coarser grid model are considerably worse (see Table 2). The average error in overestimating the tidal amplitude is 99%.

To test the OBCs in coupling coarse- and fine-resolution models, a limited-area model (LAM) of the northern part of the Adriatic Sea was produced, based on a portion of the fine grid of the Mediterranean Sea model (Fig. 6). The output from the coarse-resolution model run was interpolated to the open boundary of the LAM to create reference values of sea surface elevation η^o and velocity u_n^o for the OBCs. The results of the LAM simulations with RB, ORB, FL, and OFL conditions are shown in Figs. 7 and 8. Using the RB condition, the LAM predictions have an average error of 57% for the M_2 tidal amplitudes and 4.4% for phases. The results of simulations with ORB showed much better agreement with the observations (see Fig. 7), with an average error of 12% for amplitudes and 0.9% for phases.

The worst results in predicting tidal amplitudes occur when using the FL condition (Fig. 8). The average error is 106%; this is close to the error of the coarse grid run, the results of which were used to construct the reference values for η^o and u_n^o. The use of OFL reduced the error by half to around 47%. This has the following explanation. The use of η^o and u_n^o calculated from the coarse grid run provides too large an input of energy into the LAM when we use the standard FL condition. In the optimized version of this condition, the input from the coarse grid is corrected by the energy flux generated by the interior domain of the LAM. Calculating λ_t in OFL and ORB provides the adaptation of the boundary condition to the energy flux generated by the LAM. One can see that the results of simulations with the optimized OBCs showed much better agreement with the observations than their standard versions.

The next set of experiments was conducted with the wind forcing also included. The mean (Hellerman and Rosenstein 1983) wind stress for February was increased 10 times to get a stronger model response to the wind forcing. To establish the ''truth'' for later comparisons, the fine grid model of the Mediterranean Sea was forced for 25 days with this wind and M_2 tides. The values of the sea surface elevation and velocity on the open boundary of the LAM were stored as reference values of sea surface elevation η^o and velocity u_n^o. To test the sensitivity of the considered OBCs to the errors in functions η^o and u_n^o, we ran an experiment with the amplitudes of η^o reduced by 20% and u_n^o reduced by 50%. The results of the LAM simulations were compared with the results of the Mediterranean Sea fine grid model run. We calculated the averaged errors in predicting sea surface amplitudes and phases. These errors are 45% for amplitude and 0.8% for phase for the FL condition, 16% for amplitude and 2.6% for phase for OFL, and 22% for amplitude and 4.4% for phase for ORB. Errors in the prediction of the current ellipses for

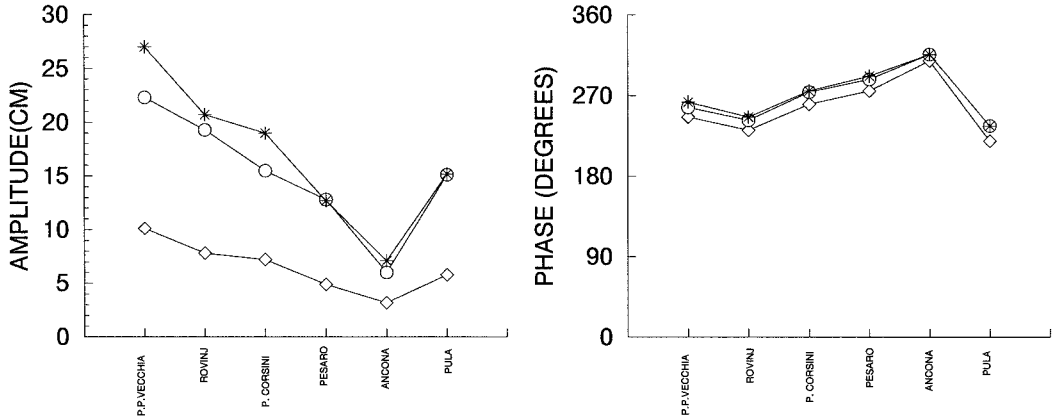

FIG. 7. Observed and model-predicted amplitudes and phases for the M_2 tide based on a simulation using a limited-area model of the northern Adriatic Sea: the circle is observed amplitudes and phases, the diamond is the results of the application of RB condition, and the star is the results of the application of ORB condition.

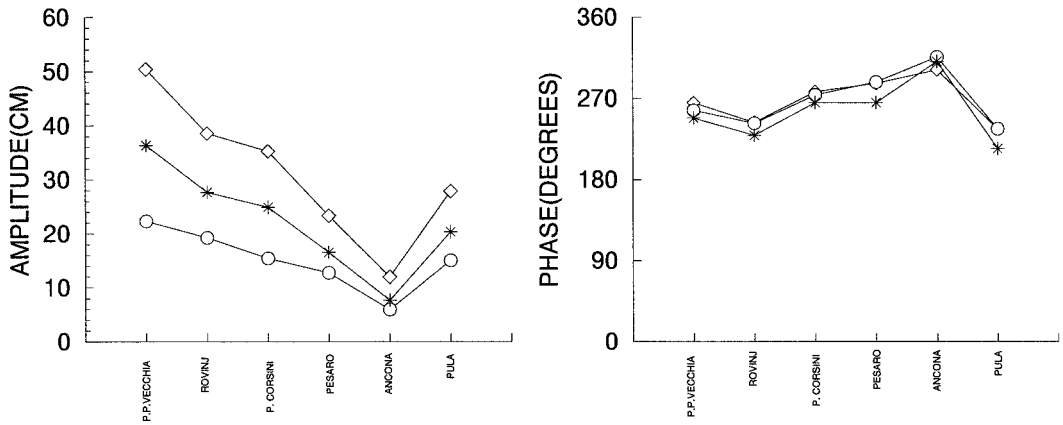

FIG. 8. Observed and model-predicted amplitudes and phases for the M_2 tide based on a simulation using a limited area model of the northern Adriatic Sea: the circle is observed amplitudes and phases, the diamond is the results of the application of FL condition, and the star is the results of the application of OFL condition.

the six tidal station locations are shown in Table 3. Optimized versions of the OBCs have an average error in predicting major axis amplitude of less than 20%. At the same time, the FL condition has an average error of 45%, which is close to the error introduced into the values of u_n^o (50%). In our next experiment, we tested the sensitivity of FL and OFL to errors in the phase of the reference velocity u_n^o. We shifted the values of the reference velocity by 3 h (which corresponds to the phase shift for M_2 tides, equaling 87°). The results are shown in Table 4. The averaged errors of the major axis predictions are 24.6% for FL and 14.8% for OFL. The predictions of phases are reasonably good for both boundary conditions.

5. Conclusions

The local data assimilation approach for specifying open boundary conditions for limited-area models is proposed. This approach provides the methodology for an optimized determination of variables on the open boundary based on available reference information about boundary values and dynamics of the model near the open boundary. The optimization problem is constrained by the physics of flux of energy through the open boundary. The reference boundary values can be derived from observations, another coarser-resolution model run, and/or from another specification of open boundary conditions. For the barotropic models, the proposed optimized open boundary conditions have a sound physical interpretation as optimized versions of well-known radiation-type open boundary conditions (Reid and Bodine 1968; Flather 1976). The results of tidal and wind-driven simulations for the idealized channel and the northern part of the Adriatic Sea show that the application of the optimized open boundary conditions reduces significantly the error of model predictions compared to the use of nonoptimized counterparts. Therefore, the proposed local data assimilation schemes of specifying open boundary conditions can provide an improvement in the accuracy in simulating model interior flow. Coupling of a coarser-resolution model and a finer-resolution limited-area model and sensitivity studies show that radiation-type open boundary conditions transmit the level of errors in the reference values into the interior domain. This can result in either overestimating or underestimating the amplitudes of sea surface elevation and velocity. But the optimized versions of these conditions correct the energy input from the reference values into the limited-area domain, and thus result in a reduction in errors. Overall, the results of simulations show that optimized open boundary con-

TABLE 3. The results of LAM simulations when amplitude of η^o is reduced by 20% and u_n^o by 50%. Relative errors in prediction of M_2 current ellipse parameters: major axis and orientation of major axis (θ).

	FL		OFL		ORB	
Station	Major (%)	θ (%)	Major (%)	θ (%)	Major (%)	θ (%)
P. P. Vecchia	45.6	1.1	18.5	0.5	23.0	0.6
Rovinj	44.9	5.0	16.6	1.9	21.5	2.4
P. Corsini	44.8	1.0	14.5	0.3	23.5	0.5
Pesaro	44.4	2.8	15.6	1.0	23.8	1.5
Ancona	43.3	2.3	18.2	1.0	30.2	1.6
Pula	46.4	6.0	17.1	2.2	20.0	2.6

TABLE 4. The results of LAM simulations when the reference velocity u_n^o was shifted by 3 h. Relative errors in prediction of M_2 current ellipse parameters: major axis and orientation of major axis (θ).

Station	FL		OFL	
	Major (%)	θ (%)	Major (%)	θ (%)
P. P. Vecchia	25.0	0.6	15.2	0.4
Rovinj	26.0	2.9	16.2	1.8
P. Corsini	22.2	0.5	9.5	0.2
Pesaro	20.6	1.3	11.7	0.7
Ancona	8.2	0.4	13.3	0.7
Pula	32.3	4.2	17.1	2.2

ditions can be used to force barotropic models or the barotropic mode of three-dimensional models (such as the Princeton Ocean Model). Our future research will be focused on extending the proposed local data assimilation techniques to the baroclinic case.

Acknowledgments. We would like to acknowledge the essential support of this work by Dr. J. K. Lewis. We are also thankful to Dr. A. F. Blumberg for stimulating comments. The comments of the anonymous reviewers were very helpful in improving the manuscript. This work was supported by a research grant from the Office of Naval Research to the Center for Ocean and Atmospheric Modeling, University of Southern Mississippi.

APPENDIX

Regularization of Optimized Open Boundary Conditions

Below we describe the approach to choose the value of the regularization parameter γ. We introduce the following notation:

$$\mu = \frac{\gamma}{g^{1/2} \int_\Gamma H^{3/2}(u_n - u_n^o)^2 \, ds}, \tag{A1}$$

and we will discuss the value of the nondimensional parameter μ. Suppose that the sea surface elevation η_{ex} is a solution of the optimization problem when P_t and u_n are the exact values for the energy flux and velocity. We do not know the function η_{ex}, but we have the function $\eta(\mu)$ from (8) and (9). Some norm of the product $\mu\partial\eta/\partial\mu$ [corresponding to the first member of the Taylor series of the difference between $\eta(\mu)$ and η_{ex}] can be used to estimate the difference between $\eta(\mu)$ and η_{ex} and to estimate the optimal value of μ and γ. Let us introduce the following norm:

$$\varphi^2 = \int_\Gamma g^{3/2} H^{1/2} \left(\mu \frac{\partial \eta}{\partial \mu} \right)^2 ds.$$

According to (A1), we have

$$\varphi^2 = \frac{P_t^2}{g^{1/2} \int_S H^{3/2}(u_n - u_n^o)^2 \, ds} \frac{\mu^2}{(1 + \mu)^4}. \tag{A2}$$

Let us introduce the normalized distribution function:

$$f(\mu) = \frac{\varphi^2(\mu)}{\int_0^\infty \varphi^2(\mu) \, d\mu},$$

which is, according to (A2), equal to

$$f(\mu) = 3\frac{\mu^2}{(1 + \mu)^4}.$$

We choose the value for μ according to the maximum entropy method:

$$\max_\mu [-f(\mu) \ln f(\mu)]. \tag{A3}$$

In this case, by maximizing entropy over all values of μ, we are picking one that makes the fewest unnecessary assumptions (most cautious hypothesis). The solution for (A3) is

$$\mu = 1 \tag{A4}$$

or

$$\gamma = g^{1/2} \int_S H^{3/2}(u_n - u_n^o)^2 \, ds. \tag{A5}$$

REFERENCES

Bennett, A., 1992: *Inverse Methods in Physical Oceanography.* Cambridge University Press, 346 pp.

——, and B. S. Chua, 1994: Open-ocean modeling as an inverse problem: The primitive equations. *Mon. Wea. Rev.*, **122,** 1326–1336.

Blumberg, A., and G. L. Mellor, 1987: A description of a three-dimensional coastal ocean circulation model. *Three Dimensional Coastal Models*, N.S. Heaps, Ed., Coastal and Estuarine Sciences, Vol. 4, Amer. Geophys. Union, 1–16.

Davies, A. M., and J. Lawrence, 1994: A three-dimensional model of the M_4 tide in the Irish Sea: The importance of open boundary conditions and influence of wind. *J. Geophys. Res.*, **99,** 16 197–16 227.

Flather, R. A., 1976: A tidal model of the northwest European continental shelf. *Mern. Soc. Roy. Sci. Liege, Ser.* 6, **10,** 141–164.

Hellerman, S., and M. Rosenstein, 1983: Normal monthly wind stress over the world ocean with error estimates. *J. Phys. Oceanogr.*, **13,** 1093–1104.

Oey, L.-Y., and P. Chen, 1992: A model simulation of circulation in the north-east Atlantic shelves and seas. *J. Geophys. Res.*, **97,** 20 087–20 115.

Officer, C. B., 1976: *Physical Oceanography of Estuaries and Associated Coastal Waters*, Wiley and Sons, 456 pp.

Oliger, J., and A. Sundstrom, 1978: Theoretical and practical aspects of some initial boundary value problems in fluid dynamics. *SIAM J. Appl. Math.*, 35(3), 419–446.

Parker, R. L., 1994: *Geophysical Inverse Theory.* Princeton Press, 386 pp.

Reid, R. O., and B. R. Bodine, 1968: Numerical model for storm surges in Galveston Bay. *ASCE, J. Water W. Harbors. Coastal Eng. Div.,* **94,** 33–57.

Sabatier, P. C., Ed., 1987: Basic concepts and methods of inverse problems. *Basic Methods of Tomography and Inverse Problems,* P. C. Sabatier, Ed., Adam Hilger, 471–643.

Seiler, U., 1993: Estimation of the open boundary conditions with the adjoint method. *J. Geophys. Res.,* **98**(C12), 22 855–22 870.

Shulman, I., and J. Lewis, 1994: Modeling open boundary conditions by using the optimization approach. TR-1/95, Center for Ocean and Atmospheric Modeling, University of Southern Mississippi, 13 pp. [Available from Institute of Marine Sciences, University of Southern Mississippi, Bldg. 1103, Room 249, Stennis Space Center, MS 39529.]

——, and ——, 1995: Optimization approach to the treatment of open boundary conditions. *J. Phys. Oceanogr.,* **25,** 1006–1011.

Zou, X., I. M. Navon, M. Berger, P. K. Phua, T. Schlick, and F. X. LeDimet, 1993: Numerical experience with limited memory quasi-Newton methods for large-scale unconstrained nonlinear minimization. *SIAM J. Optimization,* **3** (3), 582–608.